LOCAL STRESS BEHAVIOR AT CLOSED RIB TO CROSSBEAM CONNECTIONS IN ORTHOTROPIC STEEL BRIDGE DECKS

K. KATO[1*], T. HANJI[1†], K. TATEISHI[1], S.M. CHOI[1] and S. HIRAYAMA[2]

[1]*Department of Civil Engineering, Nagoya University, Japan*
[2]*Japan Bridge Association, Japan*

ABSTRACT

A large number of fatigue cracks have been reported at the connection between longitudinal closed ribs and cross-beam webs in orthotropic steel decks because of high stress concentrations due to complicated local deformations of the rib and the web. In this study, the local stress behaviors around the weld end adjacent to the cross-beam cutout were analytically investigated. Finite element analyses were conducted by using a full scale model of an actual bridge, where plenty of cracks were detected around the cross-beam cutout, to investigate the deformation modes causing the cracks. Then, the effective cutout configurations to reduce the crack-inducing local stresses were investigated by comparing the local stress in different cutout types.

Keywords: orthotropic steel deck, longitudinal rib to cross-beam connection, cutout detail, local stress.

1. INTRODUCTION

Orthotropic steel decks are often applied to viaducts in urban area. Since the orthotropic steel deck is a thin-walled structure and supports wheel loads directly, the local deformation unconsidered in the design phase occurs easily due to heavy trucks. Recently, fatigue cracks caused by the local deformation have been reported in the orthotropic steel deck, especially at connections between longitudinal closed ribs and cross-beam (or transverse rib) webs, a large number of cracks have been detected, which account for approximately 40% of the whole cracks in the orthotropic steel desk in Japan (Japan Society of Civil Engineers 2010). Therefore, it is necessary to develop countermeasures against the crack.

A lot of researches on the fatigue crack around cutouts in the cross-beam web have been conducted. For example, a cutout configuration to reduce the stress concentration around the cross-beam web cutout has been suggested (Katsumata et al. 1999; Katsumata et al. 2000), focusing on the unique longitudinal ribs in rational orthotropic steel decks. It might be possible to apply those ways to the typical longitudinal ribs, however it has not been carefully investigated yet.

* Presenter: Email: katou.keito@c.mbox.nagoya-u.ac.jp

† Corresponding author: Email: hanji@civil.nagoya-u.ac.jp

In this study, finite element analyses were carried out to investigate the local stress characteristics around the weld end adjacent to the cross-beam web cutout. A full scale model of an actual bridge, where plenty of cracks were detected around the cutout end, was analyzed to figure out the local deformation modes causing the cracks. Then, the effective cutout configurations to reduce the crack-inducing local stress were investigated by comparing the local stresses in different cutout types.

2. TARGET BRIDGE

The bridge used in this study is a three-span continuous double box-girder bridge with orthotropic steel deck as shown in **Figure 1**, which was opened in 1978. In this bridge, the traffic volume per day of whole line is approximately 80,000 and the large vehicle ratio is about 15%.

This study focused on the connection between the longitudinal closed rib and the transverse rib located just beneath a truck wheel which is circled in **Figure 1(b)**. The detail of the connection is indicated in **Figure 1(c)**. At the target weld end in this connection (see in **Figure 1(c)**), the fatigue crack was actually detected in the web of the transverse rib.

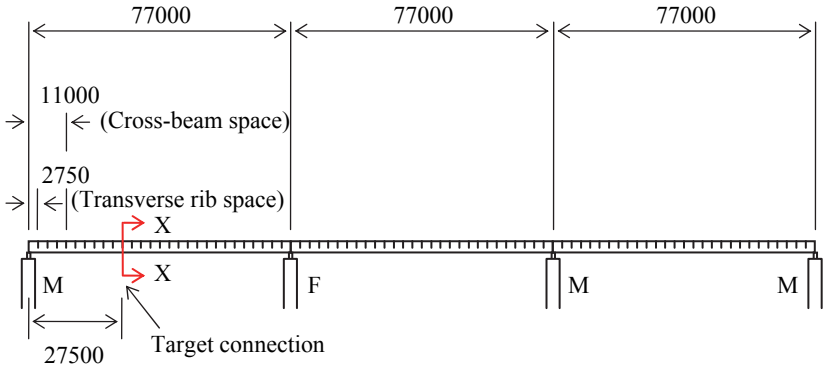

(a) Overall view

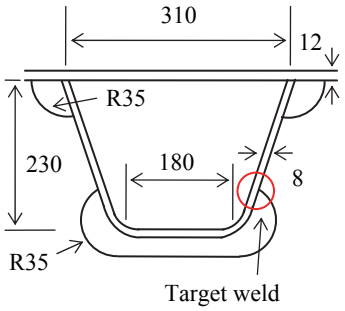

(c) Detail of connection

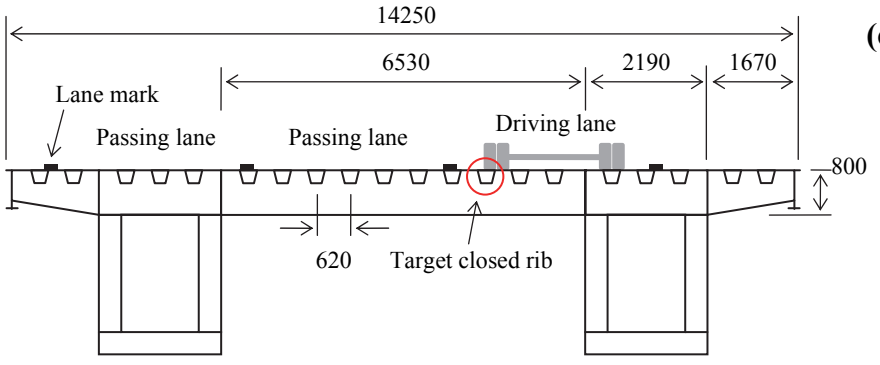

(b) X-X section

Figure 1: Target bridge (unit: mm)

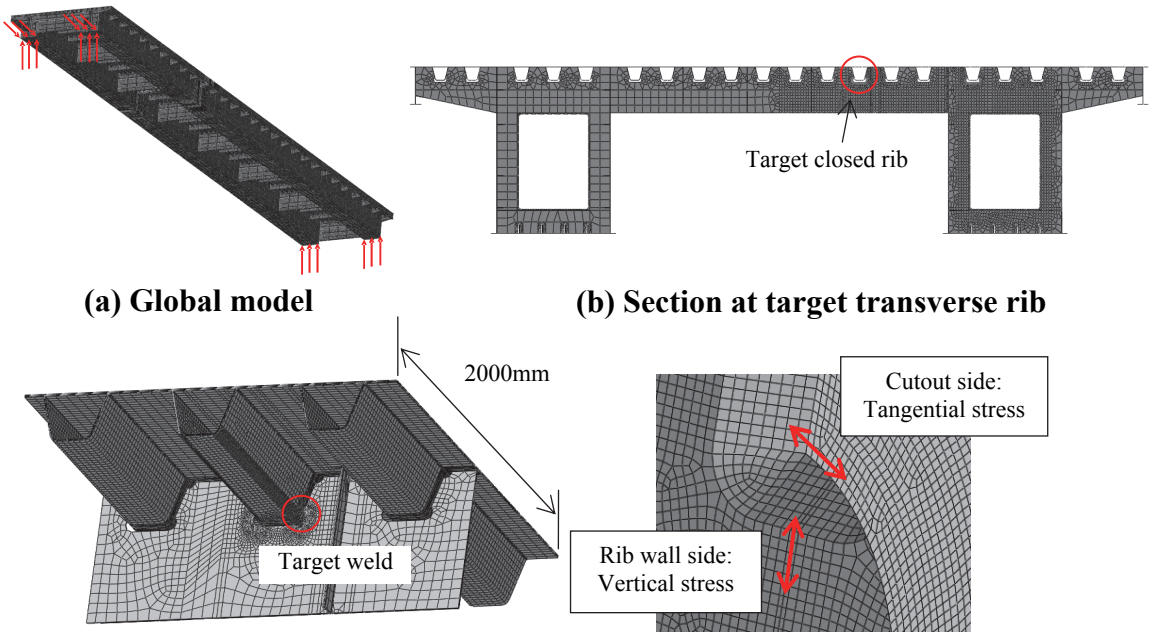

(a) Global model **(b) Section at target transverse rib**

(c) Sub model around target weld end of cutout

Figure 2: FE model

3. INVESTIGATION ON LOCAL DEFORMATION CAUSING FATIGUE CRACKS

3.1. Finite element model

A finite element model is shown in **Figure 2**. ABAQUS v6.10 was used for the analysis. In order to evaluate the local stress behavior, the sub-modeling technique was employed. As for the global model, one span in the longitudinal direction including the target transverse rib was modeled with shell elements (see in **Figure 2(b)**). As shown in **Figure 2(c)**, around the target weld end was created with solid elements to simulate the weld bead in detail, which was used as the sub model. The elements around the weld end were uniformly divided at the same size (about 1mm×1mm×1mm). The weld root was also created in the weld bead. In the model, the pavement was not considered. The Young's modulus and Poisson's ratio were 200GPa and 0.3, respectively.

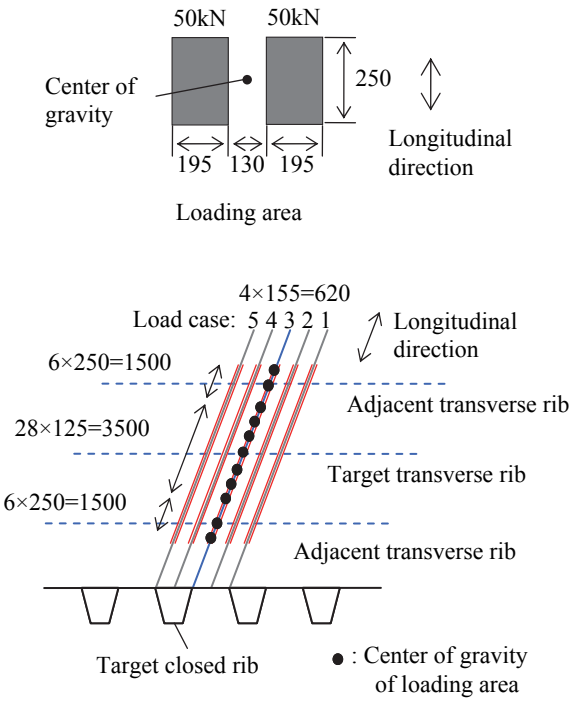

Figure 3: Loading patterns

Loading patterns simulating a single axle load composed of two truck wheel loads are illustrated in **Figure 3** (Inokuchi et al. 2011). The load was applied along five passes in the longitudinal direction

(Case 1 to Case 5). The interval of each pass is 155mm. These load passes would be enough to simulate the scatter of the actual truck wheel locations (Takada et al. 2009). Longitudinal length of each pass is 6500mm in which 41 loading points exist.

3.2. Local stress and deformation behavior

In this study, the local stress is defined as the stress of elements located along the weld toe in the closed rib wall side and in the cutout side (see in **Figure 2(c)**). The local stress behaviors in each load pass are shown in **Figure 4** and **5**. The local stress of the element indicating maximum stress fluctuation is picked out in the graph. As shown in **Figure 2(c)**, a vertical stress component was used for the local stress in the rib wall side, and the tangential stress component was used for that in the cutout side. The local stress in the rib wall side shown in **Figure 4** is related to the cracks in the closed rib wall starting from the weld end at the cutout, and the local stress in the cutout side shown in **Figure 5** is related to the cracks in the transverse rib web starting from the weld end. In the graph, the membrane stress and the bending stress calculated from the local stress are separately indicated.

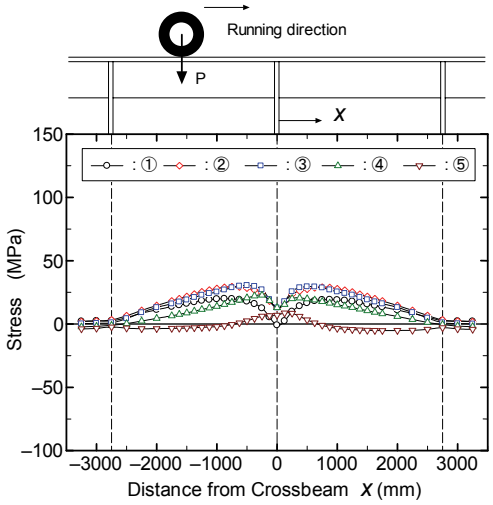

(a) Membrane stress

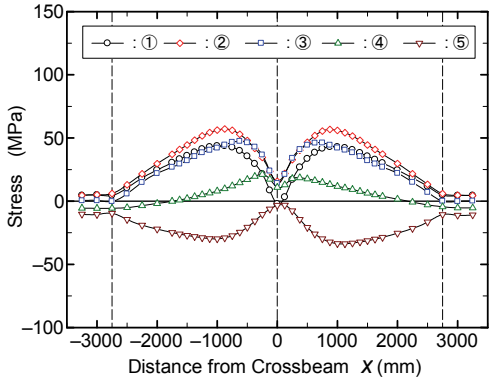

(b) Bending stress

Figure 4: Closed rib wall side

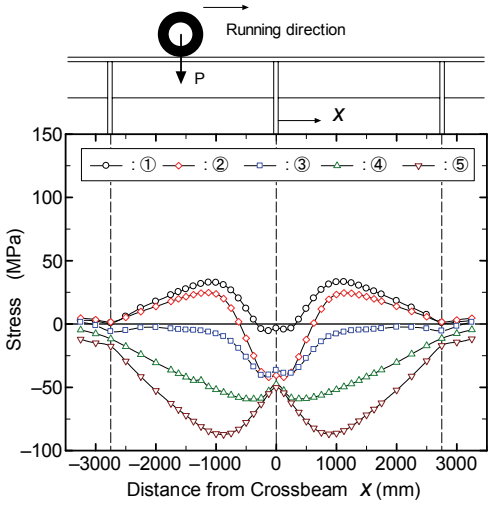

(a) Membrane stress

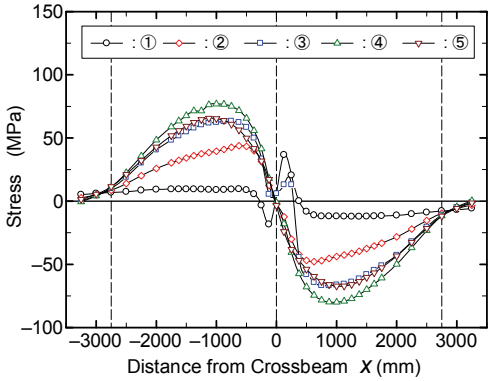

(b) Bending stress

Figure 5: Cutout side

The fluctuation range of the local stress in the cutout side is larger than that in the closed rib wall side. This result can support the actual cracking site in the bridge and mean that the magnitude of the local stress obtained from the analysis is correlated to the fatigue performance of the connection.

In the closed rib wall side, the bending stress range is dominant, and the fluctuation range of the bending stress becomes the maximum in case of load case 2. The deformation mode at the maximum stress is shown in **Figure 6(a)**. When acting the load eccentrically from the rib, the rib bottom deforms transversely causing the high local stress at the weld toe in the rib wall side.

In the cutout side, the magnitude of membrane stress and bending stress are similar. The fluctuation range of the membrane stress is relatively large in case of load case 2 and 5. Load case 4 is the case that the bending stress range becomes the maximum. The deformation mode when the bending stress is the maximum is indicated in **Figure 6(b)**.

Figure 6(a) implies that the high bending stress in the closed rib and the high membrane stress in the transverse rib occur because the transverse rib web rigidly constrains the transverse deformation of the closed rib bottom. **Figure 6(b)** implies that the out-plane deformation of the transverse rib web is caused by the vertical deformation of the longitudinal rib, leading to the bending stress at the weld end in the cutout side.

Based on the results, in order to reduce the local stress around the cutout end, it may be effective to constrain the transverse deformation of the rib bottom, or to improve the cutout configuration for transferring the stress smoothly from the wall of the closed rib to the web of the transverse rib.

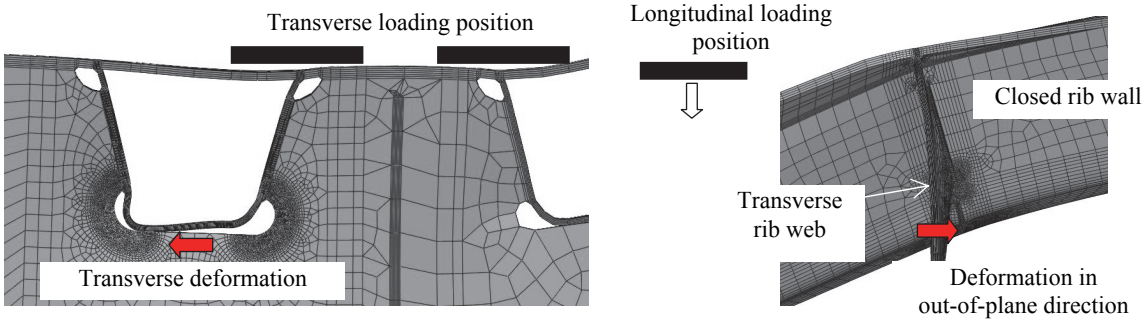

(a) Transverse deformation of closed rib **(b) Deformation of transverse rib**

Figure 6: Deformation modes causing maximum local stresses (×500)

4. EFFECT OF CUTOUT CONFIGURATIONS ON LOCAL STRESS

The effect of the cutout configurations on the local stress behavior was investigated by using the same analysis model shown in the previous chapter.

4.1. Cutout types

The cutout types taken up in this study are summarized in **Figure 7**. The dimension of the closed rib is the same in every cutout type, which is shown in **Figure 1**. Type A is the same configuration in

the previous chapter. Types B and C are the standard cutout configuration shown in design guidelines in Japan and Europe, respectively. The differences from Type A to C are the radius and depth of the cutout. Type D is the configuration that the closed rib bottom is connected to the transverse rib to constrain the transverse deformation of the rib bottom. Type E is derived from a design concept of the Bronx Whitestone Bridge (Camo and Ye 2004), in which ribs are installed inside the closed rib and the cutout ends are smoothly finished that may be able to transfer the stress smoothly from the closed rib to the transverse rib. In this study, Type F which is derived from Type E was also suggested. In Type F, the inner ribs are removed and the cutout end is extended below hoping for a similar effect to the inner rib. The cutout end in Type F is as-welded condition (not finished as Type E).

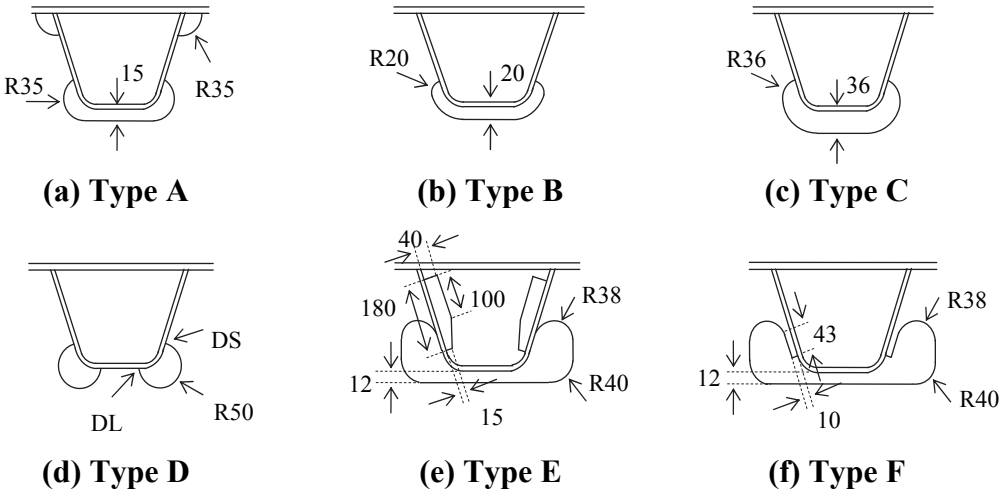

Figure 7: Cutout types (unit: mm. Weld leg sizes in all types are set to be 6mm)

The relation between the local stress and the cutout types was investigated by changing only cutout configuration in the sub model part in **Figure 2(c)**. The element sizes around the cutout and the inner rib end are almost the same in all cutout types, which are 1mm×1mm×1mm. Thus, it is possible to make relative comparison of the local stresses throughout the models. Load cases 1 to 5 illustrated in **Figure 3** were applied.

4.2. Deformation of longitudinal rib

The deformation modes when the maximum local stress occurs around the weld end of the cutout are shown in **Figure 8**. The deformation modes are similar in Type A, B and C. In Type D, the closed rib deforms locally in the cutout. It seems that the deformation causes the local stress concentration at the rib bottom as well as the rib wall. The deformation mode in Type E is similar to that in Type F, where the smooth deformation can be seen from the rib wall to the cutout. Therefore, the cutout configuration such as Type D, E, and F may be able to reduce the local stress, however in Type D, it is necessary to pay another attention to the local stress behavior at the rib bottom.

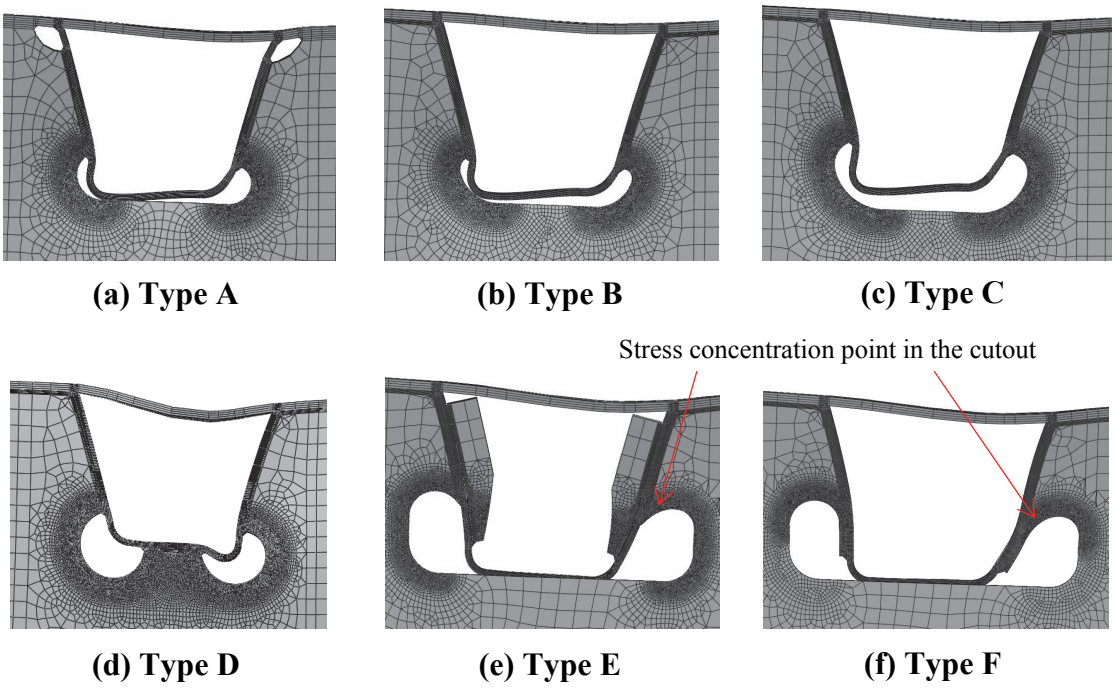

(a) Type A **(b) Type B** **(c) Type C**

(d) Type D **(e) Type E** **(f) Type F**

Figure 8: Deformation modes causing maximum local stress in different cutout types (×500)

4.3. Comparison of local stress range

The fluctuation ranges of the local stress were calculated in each cutout type when applying the load cases 1 to 5, and then the maximum ranges were compared between the cutout types. In Type D, the stress concentrations occurred at two weld ends of the cutout (at the rib wall and the rib bottom), thus this study focused on both the rib wall side and the rib bottom side, which are called DS and DL (see in **Figure 7(d)**), respectively. In type E, the stress at the end of the inner rib was used as the local stress in the rib wall side. And as for the local stress in the cutout side in Type E and F, the stress concentration points moved from the weld end to the arc of the cutout as shown in **Figure 8**, therefore the maximum stress range along the arc of the cutout was used for comparison.

The comparison of the local stresses is shown in **Figure 9**. In Type A to C, there is little difference in the rib wall side, on the other hand the local stress range in the cutout side is decreasing from Type A to C. This might be due to the depth of the cutout. In Type D, the local stress reduces at DS, while the stress at DL becomes much larger. As for Type E, the local stress decreases compared to Type A to C. The same stress reduction can be seen in Type F which has no inner ribs and no finishing of the cutout end.

The analysis results indicate a possibility that the cutout types such as Type E and F could be one of the effective countermeasures against the cracks around the connection between the longitudinal closed rib and the transverse rib web, although further investigation is required for their detail configuration.

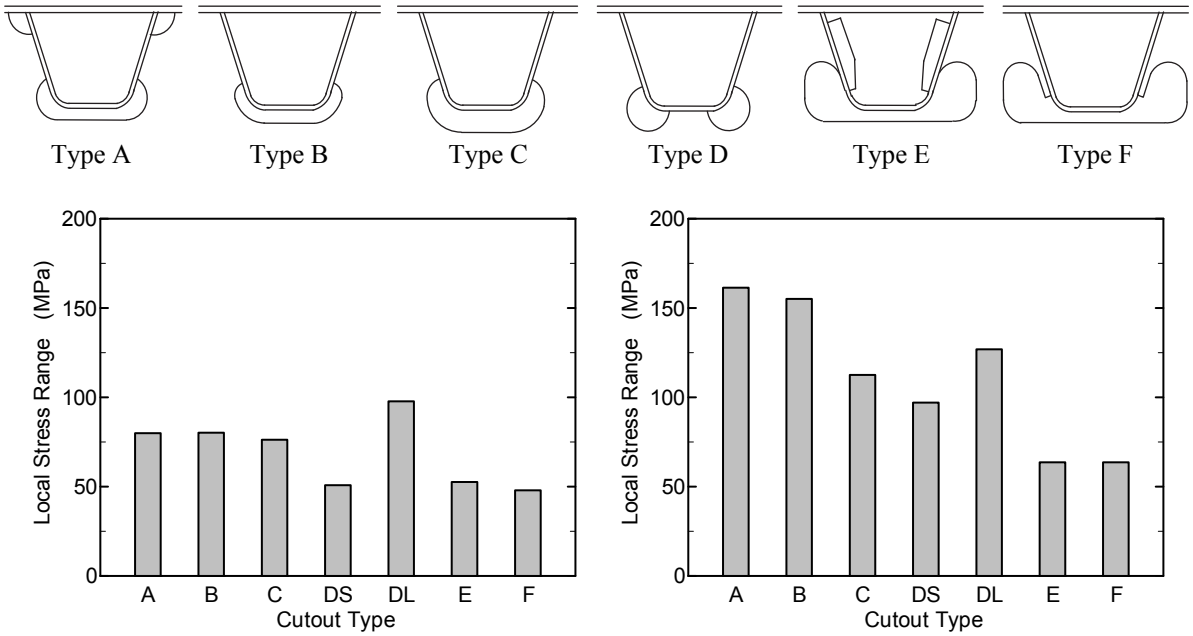

(a) Closed rib wall side **(b) Cutout side**

Figure 9: Comparisons of local stress ranges

5. CONCLUSIONS

In this study, the full scale model of the actual bridge was analyzed to clarify the local stress and deformation causing the cracks from the weld end adjacent to the cross-beam web cutout. The analysis results indicated that it may be effective to constrain the transverse deformation of the rib bottom, or to improve the cutout configuration for transferring the stress smoothly from the longitudinal rib to the transverse rib for reducing the local stress around the cutout. Then, the effective cutout configurations to decrease the crack-inducing deformations were investigated by comparing the local stress behaviors in different cutout types. As a result of the analysis, ideas to reduce the local stress around the cutout were presented.

REFERENCES

Camo S and Ye Q (2004). Design and testing for the orthotropic deck of the Bronx Whitestone bridge, Proceedings of the 2004 Orthotropic Bridge Conference, pp.616-624.

Inokuchi S, Uchida D, Hirayama S and Kawabata A (2011). Evaluation method for fatigue life of welding joint between deck plate and U-shaped rib in orthotropic steel decks. Journal of JSCE A1, 67(3), pp.464-476.

JSCE (2010). Fatigue of orthotropic steel bridge deck.

Katsumata M, Ogasawara T, Machida F, Kawase A and Mizoe Y (1999). Local stress of trapezoidal ribs to floor beams joint in rational orthotropic steel decks. Journal of Structural Engineering, JSCE, 45A, pp.1241-1252.

Katsumata M, Ogasawara T, Machida F and Mizoe Y (2000). Structual detail's experimental study regarding a simplified orthotropic steel deck's trapezoidal ribs and floor beam intersections. Journal of Structural Engineering, JSCE, 46A, pp.1233-1240.

Takada Y, Kishiro M, Nakashima T and Usui K (2009). Fatigue failure assessment of actual-working load and run location on orthotropic steel deck applied in BWIM. Journal of Structural Engineering, JSCE, 55A, pp.1456-1467.